

# Geometric Wavelength for Monitoring Dynamic Changes in Repolarization Caused by Time-Varying Parameters

Ariane Saliani<sup>1,2</sup>, Narendra Shivaraman<sup>1,2</sup>, Vincent Jacquemet<sup>1,2</sup>

<sup>1</sup> Université de Montréal, Montréal, Canada

<sup>2</sup> Hôpital du Sacré-Cœur de Montréal, Montréal, Canada

## Abstract

*The autonomic nervous system modulates atrial activity, notably through acetylcholine (ACh) release. This time-dependent action may alter the dynamics of atrial arrhythmia, and in particular its wavelength. Wavelength is a critical factor that determines the vulnerability to reentry. It represents the spatial extent of refractory periods and may be estimated as the product of action potential duration and conduction velocity. When electrophysiological properties vary in space and/or time, and when conduction is anisotropic, that estimate may be inaccurate.*

*We assessed an instantaneous geometric measure of wavelength applicable to monitoring the effect of externally-driven variations in ACh concentration at a shorter time scale than action potential duration. The method was applied to quantify the hysteresis in wavelength caused by release and degradation of ACh.*

## 1. Introduction

Cardiac arrhythmias are often observed as multiple self-sustained excitation waves propagating throughout the cardiac muscle [1]. The wavelength of these reentries represents the distance the depolarization wave travels during the functional refractory period and is often estimated as the product of action potential duration and conduction velocity. This measure will be referred to as the electrophysiological wavelength (EWL). A decrease in wavelength, either by action potential shortening or by slow conduction is a determinant of vulnerability to arrhythmia [2, 3]. The rationale is that if the wavelength becomes shorter than the length of a circuit, a reentry along that circuit is possible [4].

The definition of EWL relies on homogeneity assumptions to estimate the spatial extent of the wavelet from local measurements. In the presence of repolarization gradients, slow conduction zones or anisotropy, these homogeneity assumptions are not verified.

Mathematical approaches have been proposed to calcu-

late a geometrical wavelength (GWL) that measures the actual spatial extent of depolarization wavelets, thus offering a more complete description of the dynamics [5]. In a uniform isotropic medium, GWL is essentially equivalent to EWL, but has the advantage of providing an instantaneous measure. In contrast, EWL can only be determined at the end of repolarization. If membrane properties are changing at a time scale shorter than a heartbeat, the effects on repolarization will instantaneously reflect on the wavelength. The challenge is then to monitor the time evolution of wavelength.

Dupraz et al. [5] investigated the monitoring of wavelength in tissues with functional heterogeneities. In this paper, we explore the effect of time-dependent repolarization-related parameter variations on wavelength using reentries in a simple ring model of acetylcholine (ACh) release and degradation.

## 2. Methods

### 2.1. Simulated reentry in a ring

A ring model of canine atrial tissue (4 cm diameter, 628 cells, space step 0.02 cm) was created. Membrane kinetics was formulated using the Ramirez et al. model [6] with the addition of an ACh-dependent  $K^+$  current from Kneller et al. [7]. Tissue conductivity was 7 mS/cm, leading to a baseline conduction velocity of 80.5 cm/s. A reentry was initiated in the ring in the absence of ACh. The simulation was run during 10 s until a stable steady state regime was reached.

### 2.2. Time-dependent ACh profile

To study the effect of time-dependent variation in membrane properties on wavelength, a pre-defined spatially-uniform temporal profile of ACh concentration was specified. After a stable reentry was established in baseline condition, the protocol consisted of an ACh release phase and an ACh degradation phase, both lasting 2 s. The evolution

of ACh concentration was defined as [8]:

$$\text{ACh}(t) = \begin{cases} 0 & \text{if } t \leq t_0 \\ \text{ACh}_{\max} \frac{1 - e^{-(t_0 - t)/\tau}}{1 - e^{-(t_0 - t_1)/\tau}} & \text{if } t_0 < t \leq t_1 \\ \text{ACh}_{\max} e^{-(t_1 - t)/\tau} & \text{if } t > t_1 \end{cases} \quad (1)$$

where the onset and offset of ACh release were  $t_0 = 10$  s and  $t_1 = 12$  s. The simulation was stopped at  $t = 14$  s. The maximum ACh level ( $\text{ACh}_{\max}$ ) was varied between 0 and  $0.03 \mu\text{M}$  (30 steps; linear spacing). The time constant ( $\tau$ ) was the same for ACh release and degradation and ranged from 1 ms to 1000 ms (30 steps; logarithmic spacing). The hypothesized time course of ACh was inspired by studies on the effect of vagal stimulation on heart rate [9]. The choice of equal release and degradation rates was motivated by the objective of comparing the wavelength during the release and degradation phases rather than by physiological data.

In addition, reentries were simulated in tissues with constant ACh concentrations (10 s simulations) to establish the steady-state conditions. In total, there were 1150 simulations (250 steady-state +  $30 \times 30$  time-dependent ACh profiles).

### 2.3. Wavelength measurements

During each simulation, the time course of the membrane potential of all the nodes was stored every 1 ms. Depolarization and repolarization times were defined using a threshold at  $-70$  mV. For each action potential, conduction velocity and action potential duration were measured; electrophysiological wavelength (EWL) was defined as their product. EWL values were assigned to the times of *repolarization* of the corresponding action potentials to create a time series of wavelengths [5].

One single wavelet was present in the tissue at all times. Geometrical wavelength (GWL) was defined as the length of the region with membrane potentials above  $-70$  mV. Linear spatial interpolation was used to increase accuracy. This measure is instantaneous and is defined at every time instant. GWL was computed every 1 ms.

The evolution of wavelength measures was characterized by the time to 90% adaptation ( $T_{90}$ ) during ACh release and during ACh degradation.

## 3. Results

### 3.1. Reentries at steady state

Wavelength was first assessed during stable reentry at constant ACh concentration. In this situation, GWL and EWL were approximately equal. With increasing ACh concentration, action potential durations were shortened from 103 ms to 59 ms at  $0.003 \mu\text{M}$  and 35 ms at  $0.03 \mu\text{M}$

of ACh. Conduction velocity and cycle length (baseline values: 80.6 cm/s and 156 ms) varied by less than 5% as a combined result of hyperpolarization of the maximum diastolic potential and prolongation of the diastolic interval. Wavelength shortening by ACh is illustrated in Fig. 1. From its baseline value of 8.3 cm, GWL decreased to 2.9 cm at high ACh concentrations.

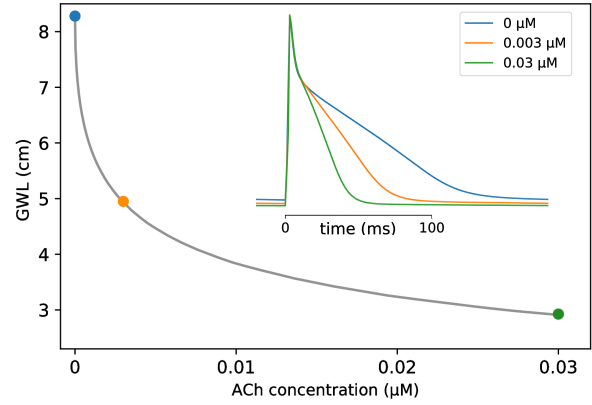


Figure 1. Steady-state geometrical wavelength (GWL) during reentry with constant ACh concentration (gray curve: 250 ACh values). Action potentials corresponding to the three colored dots are displayed in the inset.

### 3.2. Time-dependent ACh profile

Wavelength was monitored during reentry in a ring tissue with time-varying ACh concentration following Eq. (1). Figure 2 shows examples of simulations with  $\tau = 20$  and 150 ms, and  $\text{ACh}_{\max} = 0.03$  and  $0.003 \mu\text{M}$ . The predefined ACh profiles included a release and a degradation phase (panel A). The steady-state GWL time series (panel B) was defined as the steady-state GWL value from Fig. 1 corresponding to the instantaneous ACh concentration from panel A. The time evolution of GWL (panel C) and EWL (panel D) were similar and followed the evolution of ACh. Note that while GWL was computed every 1 ms, EWL could be determined only at times when a cell repolarized so the latter time series was not evenly spaced.

### 3.3. Hysteresis loops

Although the release and degradation time constants were equal, the time scale of variations in GWL was faster than ACh time constant  $\tau$  during ACh release and slower during degradation (Fig. 2). These differences were quantified using the ratio between the time to 90% adaptation ( $T_{90}$ ) and the time constant  $\tau$ . In the 900 simulations, the ratio  $T_{90}/\tau$  was  $0.58 \pm 0.21$  for the release phase

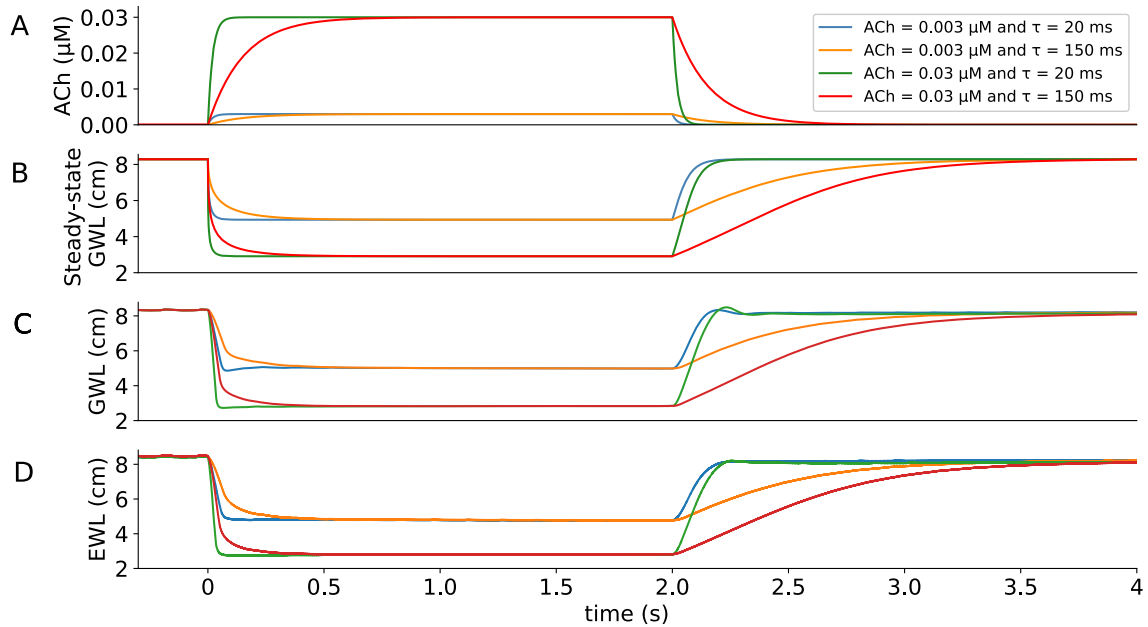


Figure 2. (A) Four examples of ACh concentration temporal profiles with different  $\tau$  and  $\text{ACh}_{\text{max}}$ . (B) Steady-state geometrical wavelength (GWL). (C) Time evolution of geometrical wavelength (GWL) and (D) electrophysiological wavelengths (EWL) in the same simulations.

and  $4.54 \pm 1.13$  for the degradation phase (paired t-test:  $p < 0.001$ ).

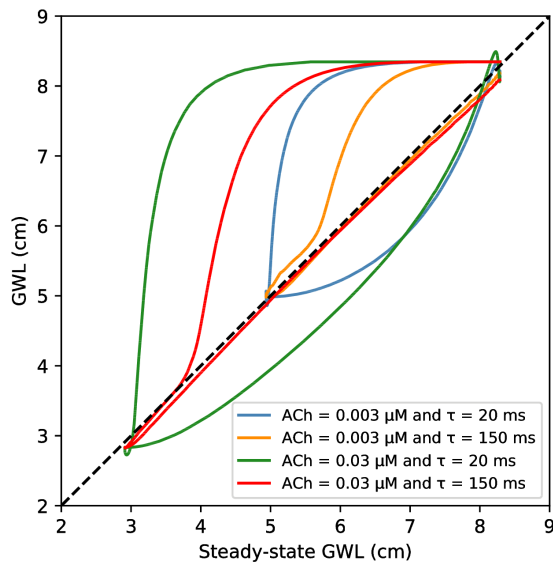


Figure 3. Hysteresis loops of geometrical wavelength (GWL) as a function of steady-state GWL. Parameters and colors are the same as Fig. 2.

This hysteresis effect can be visualized by representing GWL (from Fig. 2C) as a function of the steady-state GWL (from Fig. 2B). The resulting loops, plotted in Fig. 3, tended to cover a larger area when  $\tau$  was smaller and when

$\text{ACh}_{\text{max}}$  was larger.

The hysteresis loop areas were measured and normalized by the square of GWL range. As demonstrated in Fig. 4, this relative area was strongly and nonlinearly correlated to  $\tau$  (Spearman's rho =  $-0.99$ ), independently from ACh maximum level, and was about 40% for  $\tau = 50$  ms down to 15% for  $\tau = 1000$  ms, but appeared to tend very slowly to zero as the time constant  $\tau$  increased.

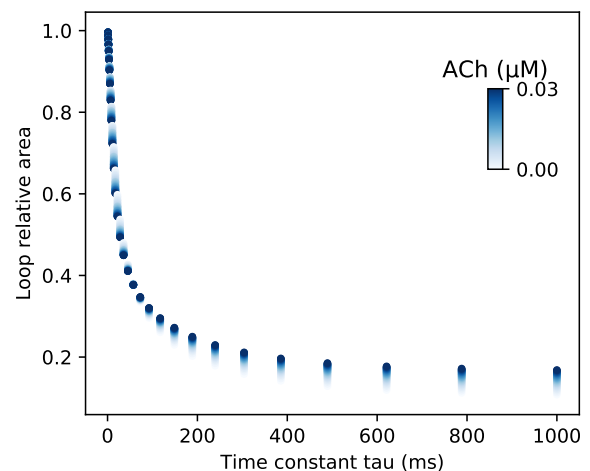


Figure 4. Loop relative area as a function of the time constant ( $\tau$ ) of ACh variation for all 900 simulations;  $\text{ACh}_{\text{max}}$  is color coded.

## 4. Discussion

GWL essentially contains the same information as EWL about the spatial extent of depolarization waves, but generalizes it to more complex conditions including heterogeneous tissue and time-varying parameters. GWL can be determined from a single snap-shot of the activity, even from the very beginning of the simulation. GWL is based on spatial maps, while EWL relies on membrane potential signal analysis. Evenly-spaced time series of GWL can be generated, which facilitates correlation analysis with respect to other variables (here, ACh concentration). Another advantage of GWL is avoiding potential inaccuracies in local conduction velocity estimation that arise when calculating EWL.

Among the limitations of GWL, its value, by definition, cannot exceed the size of the tissue. Just after the initiation of a wavefront in sinus or paced rhythm, the small depolarized region will result in a very short GWL [5]. Consequently, GWL may be used to quantify and monitor observed non-stationary dynamics of reentries but may be less appropriate than EWL as a predictor of vulnerability to arrhythmia.

## 5. Conclusion

Geometric wavelength provides an instantaneous measure to describe fast time-scale dynamic changes in refractoriness. Its application to reentries in two- and three-dimensional tissue is possible using the Dupraz et al. method [5].

## Acknowledgements

This work was supported by the Natural Sciences and Engineering Research Council of Canada (grant RGPIN-2015-05658) and by the Mitacs Globalink program.

## References

- [1] Pandit, SV and Jalife, J. Rotors and the dynamics of cardiac fibrillation. *Circ Res* 2013;12:849-862.
- [2] Rensma PL, Allesie MA, Lammers WJ, Bonke FI, Schalij MJ. Length of excitation wave and susceptibility to reentrant arrhythmias in normal conscious dogs. *Circ Res* 1988;62:395-410.
- [3] Ravelli F, Allesie M. Effects of atrial dilatation on refractory period and vulnerability to atrial fibrillation in the isolated Langendorff-perfused rabbit heart. *Circulation* 1997;96:1686-1695
- [4] Girouard SD, Rosenbaum DS. Role of wavelength adaptation in the initiation, maintenance, and pharmacologic suppression of reentry. *J Cardiovasc Electrophysiol* 2003;12:6.
- [5] Dupraz M, Jacquemet V. Geometrical measurement of cardiac wavelength in reaction-diffusion models. *Chaos* 2014;62.
- [6] Ramirez RJ, Nattel S, Courtemanche M. Mathematical analysis of canine atrial action potentials: rate, regional factors, and electrical remodeling. *Am J Physiol Heart Circ Physiol* 2000;279:H1767-1785.
- [7] Kneller J, Zou R, Vigmond EJ, Wang Z, Leon LJ, Nattel S. Cholinergic atrial fibrillation in a computer model of a two-dimensional sheet of canine atrial cells with realistic ionic properties. *Circ Res* 2002;90:E73-87.
- [8] Matene E, Vinet A, Jacquemet V. Dynamics of atrial arrhythmias modulated by time-dependent acetylcholine concentration: a simulation study. *Europace* 2014;16 Suppl 4:iv11-iv20.
- [9] Mokrane A, LeBlanc AR, Nadeau R. Transfer function analysis of vagal control of heart rate during synchronized vagal stimulation. *Am J Physiol* 1995;269:H1931-1940.

Address for correspondence:

Vincent Jacquemet  
Hôpital du Sacré-Cœur de Montréal, Centre de Recherche  
5400 boul. Gouin Ouest  
Montreal (Québec) Canada H4J 1C5  
vincent.jacquemet@umontreal.ca